

## Impact of van der Waals forces on the classical shuttle instability

T. Nord<sup>1</sup> and A. Isacsson<sup>2</sup><sup>1</sup> Department of Applied Physics, Chalmers University of Technology  
and Göteborg University, SE-412 96 Göteborg, Sweden<sup>2</sup> Department of Physics, Yale University, P.O. Box 208120, New Haven, CT 06520-8120, USA  
(Dated: February 7, 2020)

The effects of including the van der Waals interaction in the modelling of the single electron shuttle have been investigated numerically. It is demonstrated that the relative strength of the vdW forces and the elastic restoring forces determine the characteristics of the shuttle instability. In the case of weak elastic forces and low voltages the grain is trapped close to one lead, and this trapping can be overcome by Coulomb forces by applying a bias voltage  $V$  larger than a threshold voltage  $V_u$ . This allows for grain motion leading to an increase in current by several orders of magnitude above the transition voltage  $V_u$ . A signature of the process is also hysteresis in the  $I$ - $V$  characteristics.

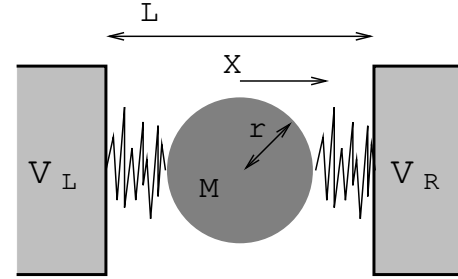
PACS numbers:

## INTRODUCTION

Nanoelectromechanical systems (NEMS) have seen a great upswing in interest over the past few years. NEMS show great promise for applications in areas such as charge detection, sensing, transistors and memory devices [1, 2, 3, 4, 5]. In many NEMS devices the interplay between electrical and mechanical degrees of freedom is crucial for the transport of charge through the system. This is due to the Coulomb forces exerted by the charge carriers which may be strong enough to cause mechanical deformations of the systems. One system where such interplay drastically changes the charge transport properties is the single electron shuttle system [6]. There a metallic grain is embedded in an elastic material between two bulk leads. Since current through that system is accompanied by charging of the grain, interplay between the Coulomb forces and the mechanical degrees of freedom can lead to self oscillations of the grain and electrons can be seen as shuttled across the gap between the leads. Experimental shuttle related work has been reported on cantilevers that work as exible tunneling contacts [7, 8, 9], single-molecule transistors [10], colloidal particle systems [11], and macroscopic shuttle systems [12]. Theoretical work has included different aspects of classical shuttle systems [6, 13, 14, 15, 16], some noise and accuracy considerations [17, 18], different aspects of quantum mechanical shuttle models [19, 20, 21, 22, 23, 24], and shuttling of Cooper pairs in a superconducting shuttle system [25, 26]. For a recent review, see Ref. [27].

When down-scaling mechanical systems into the nanometer size range, the importance of short range surface forces, such as van der Waals (vdW) forces, adhesion forces and Casimir forces, increase causing problems with for instance stiction. To make realistic models of NEMS and to design NEMS-devices, or to make optimizations of device designs, it is thus necessary to take such forces into account. In this work we report on a numerical investiga-

(a)



(b)

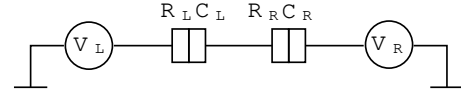


FIG. 1: Single electron shuttle. (a) A metallic grain of mass  $M$  and radius  $r$  placed between two leads separated by a distance  $L$ . The displacement of the grain from the center of the system is labelled  $X$ . The grain is connected to the leads via insulating elastic ligands. (b) Equivalent circuit of the system. The tunneling resistances and capacitances of the left and right junctions are  $R_L$ ,  $R_R$ ,  $C_L$ , and  $C_R$ . The leads are biased to the potentials  $V_L$  and  $V_R$ .

tion of the effects of vdW forces on the shuttle transport mechanism. The main result is that a new voltage scale comes into play, above which a grain trapped by the van der Waals force will be set loose due to the Coulomb interactions between the grain and the substrate. Associated with this process is a large increase in current as well as hysteretic behavior.

## MODEL SYSTEM

To be specific, we will here consider the impact of vdW forces on a mechanically soft Coulomb blockade double

junction. A schematic picture of this system is shown in Fig. 1a. A metallic grain of mass  $M$  and radius  $r$  is placed between two conductors (leads), separated by a distance  $L$ , via elastic, insulating materials (ligands). When a bias voltage  $V = (V_L - V_R)$  is applied between the leads, electron transport through the system occurs by sequential, incoherent, quantum mechanical tunneling of electrons between the leads and the grain. The system can, however, also lower its electrostatic energy by altering the grain position  $X$ . If the resulting electrostatic force is comparable to the rigidity of the insulating materials, grain displacement will occur. Thus, in this system, both electron transport and grain motion has to be taken into account.

### Electron transport

In the notion of the equivalent circuit of Fig. 1b the electrical properties of the system are characterized by resistances and capacitances  $R_L$ ,  $R_R$ ,  $C_L$ , and  $C_R$  respectively. It is important that both the tunnel resistances as well as the capacitances depend on the grain position  $X$ . The resistances depend exponentially on  $X$  as  $R_{L,R}(X) = R_0^{L,R} \exp(-X/A_{L,R})$  where  $A_{L,R}$  is the characteristic length scale for tunneling. The position dependence of the capacitances are given by

$$C_{L,R}(X) = \frac{C_0^{L,R}}{1 + \frac{X}{A_{L,R}}};$$

where  $C_0^{L,R}$  are the capacitances of the left and right junctions when the grain is at  $X = 0$ . The coefficients  $A_{L,R}$  are typical capacitance length scales for the left and right tunnel junction respectively.

Provided that the charging energy of the grain is larger than quantum for all positions of the grain, only sequential tunneling need to be considered and electrons will be localized in the leads or on the grain. This means  $E_C = \hbar^2/(2C) = e^2/2C$ . Tunneling is then well described by the "orthodox" theory of Coulomb blockade [28] from which it follows that the rates at which electrons tunnel through the left and right junctions are

$$\Gamma_{L,R}(X; V; Q) = \frac{G_{L,R}(X; V; Q)}{e^2 R_{L,R}(X)} \frac{1}{1 + \exp(-G_{L,R}(X; V; Q))}; \quad (1)$$

Here  $\beta$  is the inverse temperature and  $G_{L,R}(X; V; Q)$  is the decrease of free energy as the event  $(Q \rightarrow Q \pm e)$  occurs. The charges  $Q_L$  and  $Q_R$  denote the charges accumulated on the left and right leads and the excess charge on the grain. The free energy decrease  $G_{L,R}(X; V; Q)$  can be expressed using the equivalent circuit model of Fig. 1b [29].

### Grain motion

Considering the grain motion to be classical and one dimensional we have Newton's equation  $M \ddot{X} = F_{\text{Ext}}(X; V; Q)$  for the grain displacement. Whereas in Ref. [6] the external force  $F_{\text{Ext}}(X; V; Q)$  acting on the grain was taken to be that of a simple damped harmonic oscillator driven by a term linear in  $Q$ , we are here considering a more realistic model including an elastic force  $F_k(X)$ , a dissipative force,  $F(\dot{X})$ , an electric force  $F(X; Q; V)$  and a vdW force  $F_{\text{vdW}}(X)$  yielding the equation of motion

$$M \ddot{X} = F_k(X) + F(\dot{X}) + F(X; Q; V) + F_{\text{vdW}}(X); \quad (2)$$

The elastic force,  $F_k(X)$ , has its origin in the compressible material between the grain and the leads. Since the grain displacement resulting from the electrostatic force may lie outside the range of validity of the harmonic approximation, the nonlinearity of the elastic force has to be accounted for. In order to achieve this we have used a phenomenological potential that acts as a harmonic well with a usual spring force constant  $k$  for small displacements but that diverges as a Lennard-Jones potential (12th power) at the positions  $X_L$  and  $X_R$ . The force is thus

$$F_k(X) = \frac{a}{(X + X_L)^{13}} + \frac{b}{(X - X_R)^{13}};$$

where

$$a = \frac{k}{13} \frac{(X_0 - X_R)(X_0 + X_L)^{14}}{X_L + X_R}$$

$$b = \frac{k}{13} \frac{(X_0 + X_L)(X_0 - X_R)^{14}}{X_L + X_R};$$

This elastic force is accompanied by a dissipative force,  $F(\dot{X})$  which is, as in [6, 18], phenomenologically modeled as a viscous damping term

$$F(\dot{X}) = -\gamma \dot{X};$$

The electrostatic force,  $F(X; Q; V)$ , is given by the derivative of the electrostatic free energy  $G(X; V; Q)$

$$F(X; V; Q) = -\frac{d}{dX} G(X; V; Q)$$

$$= \frac{1}{2} \frac{dQ_L}{dX} V_L + \frac{1}{2} \frac{dQ_R}{dX} V_R - \frac{1}{2} Q \frac{dV}{dX};$$

and  $Q$  and  $V_{L,R}$  can be calculated from the equivalent circuit of Fig. 1b.

The van der Waals force,  $F_{\text{vdW}}(X)$ , between the grain and the leads can be derived from a Lennard-Jones interaction potential for the individual atoms [30] in the leads and the grain respectively. For a geometry with a

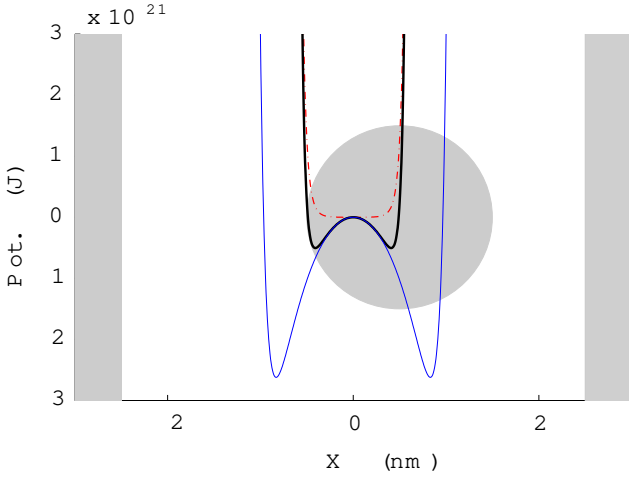


FIG. 2: Elastic potential and vdW -potential plotted together with their sum. The whole graph is superimposed on a schematic figure of the system showing the grain and the leads. The dashed curve (red) shows the elastic potential arising from the the molecular links while the thin solid line (blue) is the vdW -force curve. The total potential is shown as a thick line (black).

metallic sphere close to a substrate one ends,

$$\begin{aligned}
 F_{\text{vdW}} &= F_{\text{attr}} + F_{\text{rep}} \\
 &= \frac{H_{\text{attr}} r}{6} \frac{1}{\frac{L}{2} - r + X^2} - \frac{1}{\frac{L}{2} - r + X^2} \\
 &\quad - \frac{H_{\text{rep}} r}{180} \frac{1}{\frac{L}{2} - r + X^8} + \frac{1}{\frac{L}{2} - r + X^8} ;
 \end{aligned}$$

where  $H_{\text{attr}}, H_{\text{rep}}$  are the Hamaker constants for the attractive and repulsive parts of the force. This force has not been considered in this context before.

Equation (2) together with equation (1) for the charge transfer rates describe the dynamics of the system. The complicated form of the potentials and forces in the present model makes a detailed analytical treatment cumbersome. However, there is no problem in treating the equations numerically and the ensuing results are easily interpreted. Below we introduce a model system with a specific set of parameter values and investigate numerically the effect of incorporating adhesive surface forces on the system dynamics. The numerical investigation has been performed by doing Monte-Carlo style simulations incorporating a 4th-order Runge-Kutta routine when solving for the grain dynamics.

## RESULTS

We have considered a grain of mass  $M = 5 \cdot 10^{-23}$  kg and radius  $r = 1$  nm placed between two leads separated by a distance of  $L = 5$  nm. The elastic potential was

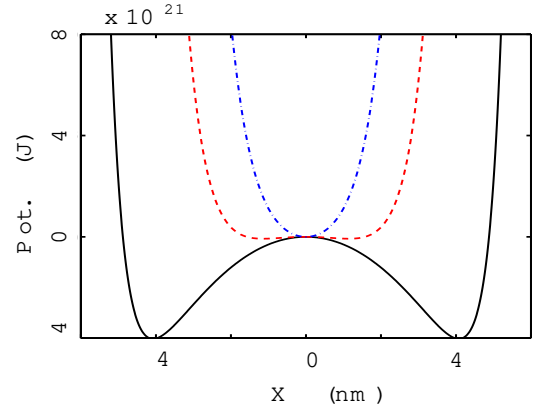


FIG. 3: The total potential arising from elastic and vdW -interactions as a function of the grain position  $X$  shown for three different values of the ligand stiffness  $k$ . The solid line (black,  $k = 0.001 \text{ Nm}^{-1}$ ) correspond to region I in Fig. 4 while the dashed line (red,  $k = 0.05 \text{ Nm}^{-1}$ ) and the dash-dotted (blue,  $k = 0.3 \text{ Nm}^{-1}$ ) correspond to the regions II and III respectively.

chosen to have a minimum in the center of the system, i.e.  $X_0 = 0$ , and to diverge at a minimum grain-lead separation of  $0.5$  nm. The tunneling resistances and capacitances corresponding to zero grain displacement were  $R_0^{L,R} = 10^{-9}$  and  $C_0^{L,R} = 10^{-18}$  F. The tunneling length was  $\lambda = 0.1$  nm and the capacitance length scale was  $A_{L,R} = 2.5$  nm. The damping constant used was  $\gamma = 10^{-13} \text{ kg s}^{-1}$ . For the vdW -interaction we have used the attractive Hamaker constant,  $H_{\text{attr}} = 4 \cdot 10^{-19} \text{ J}$  [30] and  $H_{\text{rep}}$  was chosen from dimensional considerations, to be  $10^{-72} \text{ Jm}^6$ .

In Fig. 2 the vdW -potential and the elastic potential is plotted together with their sum. The whole graph is superimposed on a schematic figure of the system showing the grain and the leads. The dashed curve (red) shows the elastic potential arising from the the molecular links while the thin solid line (blue) is the vdW -force curve. The total potential is shown as a thick line (black). It is clear that if, as is the case in our model, the insulating material does not allow the grain to come into direct contact with the leads the repulsive part of the vdW force does not come into play at all. It is also clear that the relation between the elastic force and the vdW -force determines the qualitative behavior of the total potential. Indeed, if the stiffness of the ligands is small the potential will have two stable minima whereas a stiffer conformation may have only one. The total potentials arising from different stiffnesses are shown in Fig. 3.

In Fig. 4 we have plotted numerical results for the IV -characteristics as a function of the elasticity constant  $k$ . The figure is divided into three regions. In region I, the elasticity,  $k$ , is small and the potential has two stable minima; one in the vicinity of each lead. In region III,  $k$

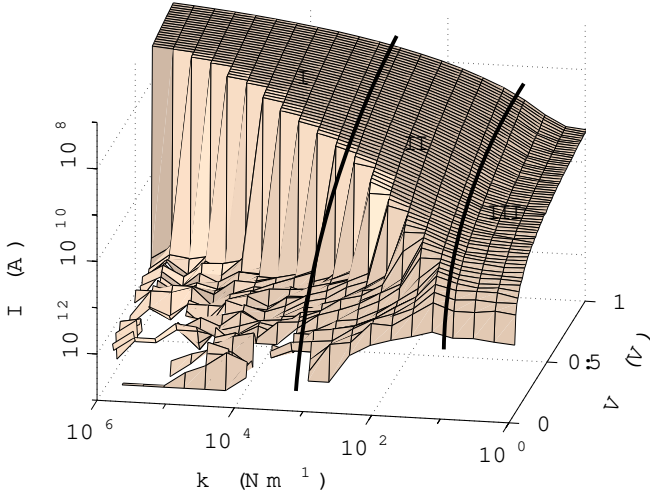


FIG. 4: The current plotted as a function of the bias voltage  $V$  and the spring constant  $k$ . The figure shows that the transition changes character from a very sharp transition in the region marked I to a more smooth transition in the region marked III. The intermediate region is marked II. In this graph all IV-curves correspond to increasing voltage sweeps which means that hysteresis effects are not shown here.

is large enough for the potential to have a single minimum in the center of the system. The potentials in Fig. 3 are representative of the different regions. The IV-characteristics in these regions differ markedly. Below we will elucidate this behavior with a mainly qualitative discussion of the dynamics, starting with the case when  $k$  is small, i.e. region I. Then moving on to discuss region III and finally we comment on the intermediate region, labelled region II in Fig. 4.

#### Small elasticity, region I

In Fig. 5a we have plotted the IV-characteristics for  $k = 0.001 \text{ Nm}^{-1}$ . The most important characteristic is the big hysteresis loop in the IV-curve. The two lower panels (b and c) of Fig. 5 show the grain position as a function of time for low and high voltages respectively. For bias voltages around zero the grain will settle in one of the two potential minima. Since the total current through the system is limited by the larger of the two tunnel resistances it will be strongly (exponentially) suppressed as compared to the situation when the grain occupies a more central position. As the voltage is increased the electrostatic force on the grain changes. The reason for this change is twofold; first, the electric field strength in the inter-electrode gap increases, and, second, increasing the bias will allow more charge to reside on the grain. When the voltage is further increased it eventually reaches a point  $V = V_0$  where the grain can escape its

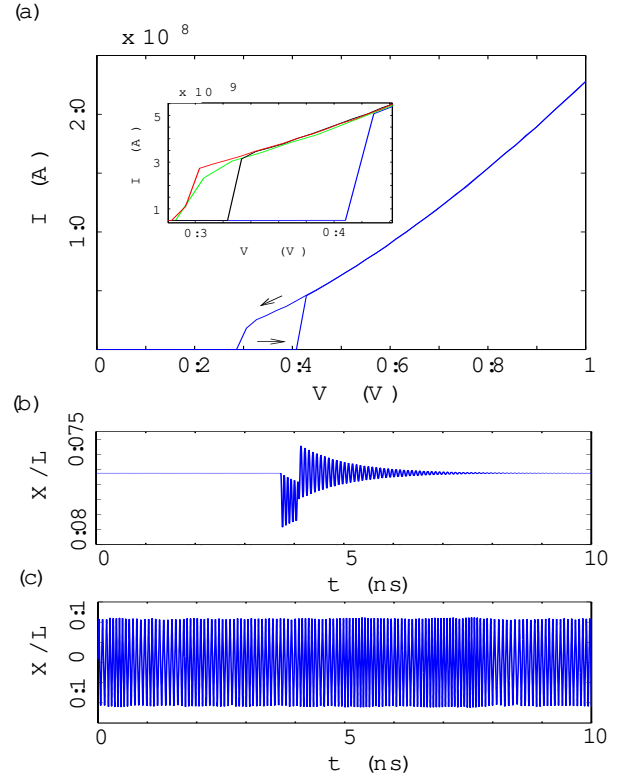


FIG. 5: (a) IV-characteristics for  $k = 0.001 \text{ Nm}^{-1}$  at zero temperature. The inset shows a closeup of the transition region. Here IV-curves for  $T = 0 \text{ K}$  for increasing (blue) and decreasing (green) voltages are shown together with IV-curves for  $T = 300 \text{ K}$  for increasing (black) and decreasing (red) voltages. (b) Position of the grain as a function of time for  $V = 0.36 \text{ V}$  in the case when the voltage is swept up. The grain sits asymmetrically in one of the potential minima caused by the strong van der Waals forces. (c) Position of the grain as a function of time for  $V = 0.36 \text{ V}$  in the case when the voltage is swept down. Since the grain is already oscillating it does not get stuck in the potential minimum and the current is still large.

locked position. In Fig. 5a this happens at a bias voltage just above  $0.4 \text{ V}$ . Below this bias the grain cannot escape its locked asymmetric position, even though, as shown in Fig. 5b, tunneling events can occur causing small movements of the grain around the local potential minimum. Above  $V = V_0$ , self oscillations of the grain appears, which causes an increase in the current by several orders of magnitude.

The transition from the locked position can occur in several different ways. In the simplest case, in the absence of thermal over-barrier activation and when the dissipation is large, the pumping due to grain motion inside the local minimum is very small, and the grain cannot escape until the minimum vanishes. However, if the minimum is shallow and the dissipation is not too high, correlation of charging and motion of the grain in the local potential minimum can lead to energy pump-

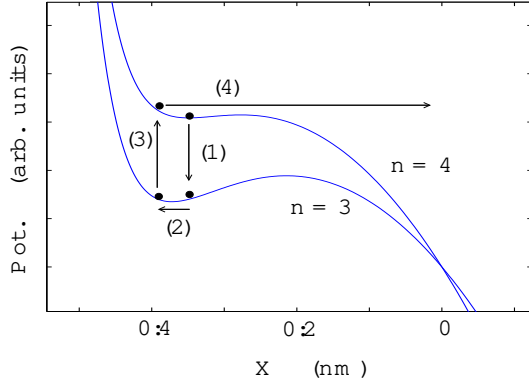


FIG. 6: Example of grain escape by a single pumping cycle. A grain initially carrying  $n = 4$  extra electrons and at rest in the local minimum of the total potential cannot escape over the barrier at low temperatures. However, a charging and motion sequence as described by the arrows (1) through (4) provides the necessary energy to overcome the barrier.

ing and grain escape. An example of such a sequence of correlated events is illustrated in Fig. 6. The figure illustrates a grain initially having  $n = 4$  extra electrons and that is positioned in the local minimum of the total potential. The numbered arrows correspond to the following events: (1) A tunneling event occurs changing the charge from  $n = 4$  to  $n = 3$ . This change in charge is associated with a corresponding change in the potential. The grain is now not positioned in the minimum of the  $n = 3$  potential. (2) The grain moves in the  $n = 3$  potential until a new tunneling event occurs. (3) A tunneling event changes the charge back to  $n = 4$ . (4) The grain, again in the potential for  $n = 4$ , now has enough energy to escape the potential well.

The main IV-curve in Fig. 5a corresponds to the case of zero temperature. In this case, the maximum charge allowed on the grain, and hence, the most "shallow potential" experienced by the grain, is determined by the bias voltage due to charging effects (Coulomb blockade). At finite temperatures, thermal fluctuations of the grain charge can cause the grain to become released at a lower voltage. In the inset of Fig. 5a a close up of the transition region for both a finite ( $T = 300$  K) and zero temperature is shown. As can be seen, the threshold where the grain escapes its locked position is considerably lowered for the high temperature case, while the remaining part of the curve remains unchanged.

To understand the hysteresis appearing in the curve consider a voltage above  $V_u$ . Provided that the dissipation is not too high a sustained oscillation of the grain between the leads results. Whether or not this oscillation occurs depends, once the grain is released, on the relation between the energy pumped by the work done by the electric field between the leads and the dissipation in the system [6, 13]. Lowering the voltage below  $V_u$

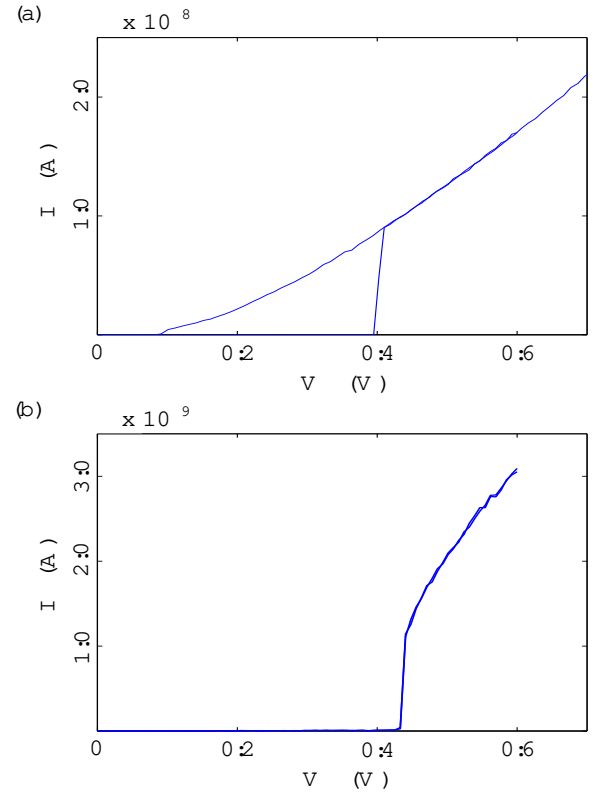


FIG. 7: The IV-characteristics of the same system as described in Fig. 5 but with different dissipation factors to investigate features of the hysteresis. In (a) the dissipation is lowered to  $\gamma = 10^{-14}$  kg s $^{-1}$  and we see that the hysteresis is bigger than in Fig. 5. In (b) the dissipation is instead increased to  $\gamma = 10^{-12}$  kg s $^{-1}$  and the hysteresis has disappeared completely.

once the grain is oscillating does then not imply that it will be stuck in one of the local minima of the potential. Hence, by changing the magnitude of the dissipation the size of the hysteresis loop varies. This is illustrated in Fig. 7 where a case with large hysteresis ( $\gamma = 10^{-14}$  kg s $^{-1}$ ) and a case with no hysteresis ( $\gamma = 10^{-12}$  kg s $^{-1}$ ) are shown. It should be noted that the current in Fig. 7a and b differ by one order of magnitude. The dynamics of the latter case, when dissipation dominates the behavior, is mainly the same as in Ref. [16] where it was further investigated.

#### Large elasticity, region III

In the limit when the elasticity dominates the short range attractive forces only one minimum results from the elastic and vdW potentials. This yields IV-characteristics belonging to region III in Fig. 4. The particular curve corresponding to  $k = 0.3$  N m $^{-1}$  is shown in Fig. 8a. In this case, as the bias voltage is increased the shuttle instability develops from the one minimum in

the potential. Sweeping the voltage down again reveals the absence of hysteresis.

It should be noted here that, although the system operates in a regime analogous to the shuttle system in Ref. [6], no steps are visible in the IV-curve even at zero temperature as would be the case if the elastic potential was purely harmonic. For a harmonic potential, increasing the bias leads to larger oscillation amplitudes at constant frequency, meaning that the grain comes closer to the lead. Since the tunnel resistance decreases exponentially with decreasing grain-lead distance the tunnel rate increases exponentially. Thus, increasing the amplitude at constant oscillation frequency implies that the grain charge has time to reach complete equilibrium with the lead. This in turn gives maximum step sharpness in the IV-characteristics [17]. The presence of the strong anharmonicity though, confining the grain to the center of the system, implies that with increasing bias the energy pumped into the vibrational degrees of freedom increases not only the amplitude but also the frequency. When the frequency increases the time spent by the grain in close contact with the lead decreases. Unless the amplitude is increased accordingly the grain charge does not have time to reach equilibrium with the lead, leading to the suppression of the steps seen in the IV-curves presented here.

Although it is hard to tell from the curve in Fig. 8a that shuttling is present, it is more obvious from Fig. 8b and Fig. 8c where the position of the grain as a function of time is shown for the voltages  $V = 0.2$  V and  $V = 1.0$  V.

#### Intermediate elasticity, region II

In the intermediate region the potential minima are not as deep as in region I (cf. Fig. 3). An interesting phenomenon can occur in this regime; As the bias voltage is raised the grain can sit in one minimum, then be pushed to the other, oscillate there for a short time, and then change side again. This behavior is shown in Fig. 9b where the position of the grain as a function of time is plotted for  $k = 0.05$   $\text{Nm}^{-1}$  and  $V = 0.1$  V.

Raising the bias, the grain switches side with increasing frequency (see Fig. 9c) until it changes side twice in each oscillation period. Since the potential is flatter in this regime, the shuttle transition occurs at a lower voltage than in region III.

#### CONCLUSIONS

We have investigated the effects of van der Waals forces on the current transport through a shuttle system. Our results show that the relative strength between these forces changes how the transition from non-shuttle to

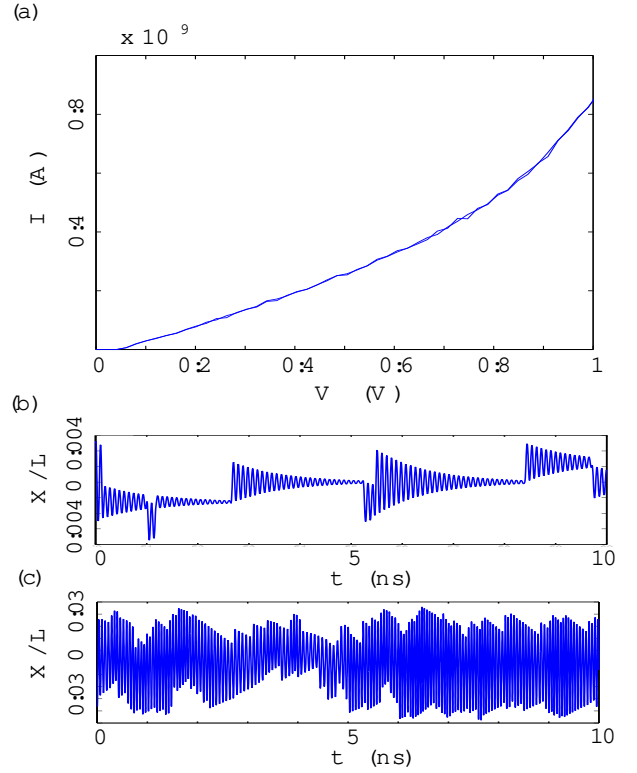


FIG. 8: (a) IV-curve for  $k = 0.3$   $\text{Nm}^{-1}$ . (b) Position of the grain as a function of time for  $V = 0.2$  V. The grain oscillates in the single minimum in the potential. The position of the minimum changes with the number of charges on the grain due to the applied electric field. (c) Position of the grain as a function of time for  $V = 1.0$  V. As the voltage is increased the grain starts to oscillate across the system.

shuttle transport occurs. In the region where the elastic force is small the transition is very sharp and there is a big hysteresis loop in the IV-curve, whereas in the region where the elastic force is big the transition is softer and there is no hysteresis. Between the two regions is a crossover region where the transition voltage is significantly lowered and where, for lower voltages, the grain alternately oscillates inside and between the minima of the potential.

#### ACKNOWLEDGMENT

We would like to thank Robert Shekhter and Leonid Gorelik for valuable discussions and useful remarks on this manuscript. One of the authors (A.J.) acknowledge financial support from the Swedish SSF through the programme QDNS and from the Swedish Foundation for International Cooperation in Research and Higher Education (STINT).

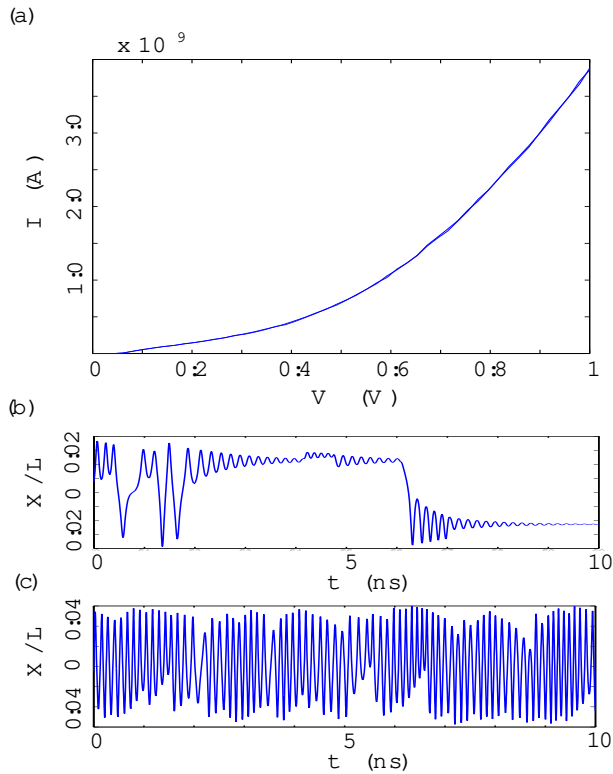


FIG. 9: (a) IV-characteristics for  $k = 0.05 \text{ nm}^{-1}$ . (b) Position of the grain as a function of time for  $V = 0.1 \text{ V}$ . For low voltages the grain oscillates in one potential minimum until a tunnel event changes its charge. It is then moved across the system to the other minimum where it oscillates until the charge changes again. (c) Position of the grain as a function of time for  $V = 0.4 \text{ V}$ . For higher voltages the grain starts to oscillate across the system.

nord@fy.chalmers.se

- [1] M. Roukes, Phys. World February, 25 (2001); Opening Lecture, 2000, Solid State Sensor and Actuator Workshop, Hilton Head, SC 6/4/2000, published in Technical Digest of the 2000 Solid State Sensor and Actuator Workshop.
- [2] P. Kim and C. M. Lieber, Science 286, 2148 (1999).
- [3] R. H. Blick, A. Erbe, H. Krommer, A. Krais, and J. P. Kotthaus, Physica E 6, 821 (2000).
- [4] T. Rueckes, K. Kim, E. Joselevich, G. Y. Tseng, C. Cheung, and C. M. Lieber, Science 289, 94 (2000).

- [5] J. M. Kinaret, T. Nord, and S. Vieira, Appl. Phys. Lett. 82, 1287 (2003).
- [6] L. Y. Gorelik, A. Isacsson, M. V. Voinova, B. Kasemo, R. I. Shekhter, and M. Jonson, Phys. Rev. Lett. 80, 4526 (1998).
- [7] A. Erbe, R. H. Blick, A. Tilke, A. Kriele, and J. P. Kotthaus, Appl. Phys. Lett. 73, 3751 (1998).
- [8] A. Erbe, C. Weiss, W. Zwirger, and R. H. Blick, Phys. Rev. Lett. 87, 096106 (2001).
- [9] D. V. Scheible, A. Erbe, and R. H. Blick, New J. Phys. 4, 86.1 (2002).
- [10] H. Park, J. Park, A. K. L. Lim, E. H. Anderson, A. P. Alivisatos, and P. L. McEuen, Nature (London) 407, 57 (2000).
- [11] K. Nagano, A. Okuda, and Y. Majima, Appl. Phys. Lett. 81, 544 (2002).
- [12] M. T. Tuominen, R. V. Krotkov, and M. L. Breuer, Phys. Rev. Lett. 83, 3025 (1999).
- [13] A. Isacsson, L. Y. Gorelik, M. V. Voinova, B. Kasemo, R. I. Shekhter, and M. Jonson, Physica B 255, 150 (1998).
- [14] A. Isacsson, Phys. Rev. B 64, 035326 (2001).
- [15] N. Nishiguchi, Phys. Rev. B 65, 035403 (2001).
- [16] T. Nord, L. Y. Gorelik, R. I. Shekhter, and M. Jonson, Phys. Rev. B 65, 165312 (2002).
- [17] C. Weiss, W. Zwirger, Europhys. Lett. 47, 97 (1999).
- [18] N. Nishiguchi, Phys. Rev. Lett. 89, 66802 (2002).
- [19] D. Boese, H. Schoeller, Europhys. Lett. 54, 668 (2001).
- [20] D. Fedorets, L. Y. Gorelik, R. I. Shekhter and M. Jonson, Europhys. Lett. 58, 99 (2002).
- [21] K. D. McCarthy, N. Prokofev, and M. Tuominen, (unpublished), cond-mat/0205419.
- [22] A. D. Armour, and A. MacKinnon, Phys. Rev. B 66, 035333 (2002).
- [23] D. Fedorets, L. Y. Gorelik, R. I. Shekhter, and M. Jonson, (unpublished), cond-mat/0212561.
- [24] T. Novotny, A. Donarini, and A.-P. Jauho, (unpublished), cond-mat/0301441.
- [25] L. Y. Gorelik, A. Isacsson, Y. M. Galperin, R. I. Shekhter, and M. Jonson, Nature (London) 411, 454 (2001).
- [26] A. Isacsson, L. Y. Gorelik, R. I. Shekhter, Y. M. Galperin, and M. Jonson, Phys. Rev. Lett. 89, 277002 (2002).
- [27] R. I. Shekhter, Y. Galperin, L. Y. Gorelik, A. Isacsson, and M. Jonson, J. Phys.: Condens. Matter 15, 441 (2003).
- [28] I. O. Kulik and R. I. Shekhter, Sov. Phys. JETP 41, 308 (1975).
- [29] D. V. Averin and K. K. Likharev, in Mesoscopic Phenomena in Solids, edited by B. L. Altshuler, P. A. Lee, and R. A. Webb (Elsevier, Amsterdam, 1991), p. 173.
- [30] J. N. Israelachvili, Intermolecular and Surface Forces (Academic Press, London, 1985).